JOURNAL OF AIRCRAFT
Vol. 41, No. 4, July–August 2004

Retrospective and Recent Examples of Aircraft Parameter Identification at NASA Dryden Flight Research Center

K. Charles Wang*
The Aerospace Corporation, El Segundo, California 90009-2957
and
Kenneth W. Iliff†
Lancaster, California 93536

A brief retrospective is presented on the development of aircraft aerodynamic parameter identification at NASA Dryden Flight Research Center, tracing its origins from the mid-1960s through recent flight examples. The maximum-likelihood output-error approach is summarized, leaving details to ample references. A partial listing is provided of flight programs at Dryden over the last 40 years that have used parameter identification to support flight testing. In particular, highlights and lessons learned within the last 12 years are described from the X-29A, F-18, SR-71, and space shuttle programs. Results show the usefulness of modeling state noise to account for uncommanded responses caused by separated and unsteady flows at high angles of attack, the importance of proper maneuver planning in reducing data scatter, and the need for multiple and repeated maneuvers to adequately characterize the estimated stability and control derivatives. Over the last 40 years, aircraft parameter identification has proven invaluable to both research and production flight vehicles in safely expanding the operational flight envelope, placard modification and removal, updating the aerodynamic database and math model, refining ground-based simulators, revising control system design, and improving handling qualities.

Introduction: 40 Years of Parameter Identification at Dryden

Precursor—Analog Matching

As with most technological advances, modern parameter estimation or parameter identification (PID) was born out of technical necessity. (Although the term "parameter identification" and acronym PID are often used to describe the subject technique, the more accurate term is "parameter estimation." For simplicity, however, the two terms are used interchangeably herein.) In the early 1960s, the NASA Flight Research Center, as it was known then, was actively engaged in flight testing of the rocket-powered X-15 and early lifting-body (M2) programs.[1,2] An important task in support of flight envelope expansion was to extract aerodynamic stability and control derivatives from measured flight data. A popular technique at the time known as analog matching[3,4] used the aircraft equations of motion programmed onto an analog computer. Potentiometers would then be adjusted to change what corresponded to stability and control derivatives until the best possible curve fit or match was obtained between the flight data and the analog simulation of the given flight maneuver. It was essentially a manual precursor to the automated PID techniques of today. Some maneuver analyses involved having to match six or seven different curves or time histories of various flight variables. Obtaining the best match to characterize the maneuver was extremely time consuming and tedious, with some analyses taking up to several weeks of human effort. Moreover, results could vary significantly from analyst to analyst depending on experience and skill.

Perfect Problem for a Computer

The digital computer age was just beginning in the early 1960s, and it became apparent that a major improvement could be achieved if a computer program could be written to perform the curve fitting of the time histories used to determine the aerodynamic derivatives (coefficients) in some mathematically consistent way. Trends from analog matching suggested that a minimization technique could automate the process. Initially, Dryden engineers Lawrence W. Taylor and Kenneth W. Iliff pursued already known regression techniques, such as linear least squares[5] and weighted least squares.[6] These methods, however, tended to give poor results in the presence of measurement noise and yielded biased estimates. Frequency response methods[7] were also popular in aircraft analysis at the time, including steady-state oscillator analysis[8] and Fourier analysis,[9] but these methods did not yield the coefficients of the differential equations. The time-vector technique[3] was also studied, but it yielded an incomplete set of coefficients, and the types of responses that could be analyzed were restricted to only simple motions. Comparisons of these early techniques[10,11] showed that a more complete method of identification was needed.

Theoretical considerations pointed to more advanced, nonlinear, iterative techniques. A technique called maximum-likelihood estimation was of particular interest. Experts from outside Dryden were consulted for their theoretical expertise in these areas. In particular, A. V. Balakrishnan[12,13] of the University of California at Los Angeles (UCLA) was very enthusiastic and subsequently worked closely with Taylor and Iliff on the problem.

By the mid-1960s, Taylor, Iliff, and Balakrishnan had developed a FORTRAN program that brought together the flight data, the mathematics describing the equations of motion, and the mathematics describing the optimization technique. [The technique that we currently call MMLE (modified maximum-likelihood estimation) was originally called least squares, but it was always confused with linear least squares (regression), and so the technique was subsequently referred to as the Newton–Raphson method, which is the method of minimization we still use today.] Using a simulator for comparison, extracted derivatives using the program (which basically minimized the error, in the least-squares sense, between the model response and the measured response) were shown to better describe the flight data than did derivatives obtained by earlier regression techniques. Flight data from the M2-F1 were used for the first successful application of the new technique, which could yield a complete set of aerodynamic coefficients. Several X-15 stability and control maneuvers were also selected for analysis and validation of the maximum-likelihood

Received 26 September 2003; revision received 18 November 2003; accepted for publication 22 November 2003.

*Project Engineer, M/S: M6-206, P.O. Box 92957. Senior Member AIAA.
†Retired. Fellow AIAA.

estimator. Its iterative nature took full advantage of the computer in terms of speed, productivity, consistency, and efficiency. These first successful results were achieved in early 1966.

The results were published in the open literature for the first time two years later in 1968 at an international conference in San Remo, Italy.[14] A companion paper was presented later that same year, which discussed results from the X-15 rocket plane, HL-10 lifting body, and XB-70 supersonic intercontinental bomber programs.[15] There was a subsequent modification to these techniques that included a priori information in the analysis.[16]

One reason for the success of the new technique was that previous research had furnished a well-defined mathematical model that adequately described the physics and phenomenology—the resulting aircraft motions, in this case. The governing mathematical differential equations were established decades before,[17,18] and the maximum-likelihood estimator was also well grounded in theory.[13,19]

The motivation for solving the aircraft parameter estimation problem using computational methods was threefold: 1) to take the tedium out of derivative extraction from the analog-matching point of view, 2) to provide a more consistent and repeatable method and reduce the uncertainty caused by variations from analyst to analyst, and 3) using an automated technique that requires the entire time history to be self-consistent also allowed for the extraction of minor (or secondary) stability and control derivatives. The last motivation was becoming increasingly important in the 1960s because a large number of aircraft either had or were planned to have closed-loop feedback control systems (or stability augmentation systems). This meant that traditional stability and control maneuvers using a single control surface pulse in doublet form were no longer possible. With feedback, the control system commanded other surfaces to move as well as the one being commanded, complicating the extraction of control derivatives. But the new technique allowed the extraction of derivatives in the presence of feedback, including second-order effects such as the rotary and weaker control derivatives.

Fitting into the Bigger Picture—Engineering Utility

The engineering utility of parameter estimation (or PID) within the context of the aircraft design and development process is worth noting. Parameter estimation enters the process through the aerodynamic database, which is initially based on wind-tunnel measurements as well as analytical and computational-fluid-dynamic predictions. The simulation resulting from that database serves as the primary tool to understanding how the vehicle flies. As flight testing begins and aerodynamic maneuvers are flown, parameter estimation is used to extract specific stability and control derivatives from the flight data. Those flight-derived stability and control derivatives are then compared to the predicted aerodynamic database, and changes are made to the database to make it more consistent with actual flight behavior. During the envelope expansion phase, PID results from previous flights feed directly into maneuver planning for subsequent PID maneuvers. Flight maneuvers can be input by the pilot or by the flight computer via preprogrammed commands. Most flight-test programs today use the latter, such that the pilot is not fighting the control system and vice versa during the maneuver. As the aerodynamic database is updated and refined with flight-derived stability and control derivatives, there is a greater harmony between what the vehicle exhibits in flight and what we have on the fixed-based simulator.

In addition, flight-derived derivatives are used to verify compliance with the original requirements and design specifications of the vehicle. The values are also used to determine flight safety, handling qualities, and overall aircraft system performance. Modifications and improvements to the flight control system are also based on the flight values. Differences between flight and prediction are analyzed together with wind-tunnel engineers to understand phenomenology. Differences can include Reynolds- or Mach-number effects, scale effects, or differences in the configuration tested and the configuration flown. This type of feedback to the designers serves the important role of assessing the predictive tools used to design the aircraft. Occasionally, the difference between the prediction and flight is so great that an aerodynamic modification is made to the vehicle prior to further flying. In addition to determining stability and control derivatives, parameter estimation has been used to determine lift and drag characteristics,[20] investigate the structural dynamics of a vehicle,[21] and, to a lesser degree, study propulsion effects.[22,23]

Spreading the Word

The original FORTRAN computer program developed at Dryden was rather crude in terms of readability and user friendliness. Programmers at Dryden tried to improve the interface to make the program more useful to others. At the time, although Langley Research Center was the lead NASA Center in terms of extraction of information from flight data, Dryden efforts were followed closely, and results were shared freely within NASA and outside NASA as well.

To facilitate distribution of the program, a "bare-bones" version of the program was created with just the basic part of the minimization and formulation of equations. The Bare Bones program, as it was known, was written in standard FORTRAN and rigorously tested so that it would run on any FORTRAN compiler. The code ran very efficiently and used relatively little memory, quickly becoming the standard "engine" of similar programs in the industry. The program was distributed to organizations such as NASA Langley, China Lake (U.S. Navy), Northrop, Boeing, North American Aviation, UCLA, and University of Southern California, with each organization adding their own user interfaces for their particular analyses.

Broad Application and Further Refinements

Taking advantage of the large variety of flight-test programs during the 1960s and early 1970s, the code was validated on many different aircraft in diverse flight regimes. One of the more interesting programs was the 3/8th-scale remotely piloted F-15 that was used for high-angle-of-attack research. A full parameter estimation analysis was done from +40 deg angle of attack to −20 deg angle of attack.[24] Another program was the Gossamer Albatross, a human-powered vehicle that was flown across the English Channel. Thus by 1980, stability and control derivatives had been extracted from vehicles flying as slow as 15 km per hour and from vehicles flying as fast as Mach 6 (X-15), including analysis in the transonic region.

The F-8 Supercritical Wing program afforded the opportunity to apply parameter estimation to determine lift and drag data.[20] The maneuvers, called push-over/pull-up maneuvers, were done faster than appropriate for the quasi-steady-state assumption, but the extracted data still agreed with data from traditional performance determination techniques.

In the late 1960s, after the maximum-likelihood technique was established at Dryden, Taylor and Iliff looked extensively at the extended Kalman filter, but found difficulties with convergence and multiple minima. The PID problem was also studied in the frequency domain, with some success. The emphasis at Dryden remained with the (time-domain) maximum-likelihood method. (After transferring to Langley in the late 1960s, Taylor did additional work on the frequency-domain application.)

Around 1970, Iliff began investigating the parameter estimation problem in which state noise is present, known technically as the nondeterministic problem.[25] The simplest example of state noise would be an aircraft flying through turbulence where the near-random "inputs" of the atmospheric forces on the vehicle are unknown.[26] The Kalman filter (not the extended Kalman filter) was used for this problem, which allowed the identification of the stability and control derivatives as well as the time history of the winds (turbulence) affecting the vehicle. The turbulence was modeled with the Dryden spectrum, which describes the amplitude of a gust or of turbulence as a function of the frequency of the gust. Use of the von Kármán spectrum was also investigated, but without obvious improvements, such that most of the analysis in this area at Dryden have all been done with the Dryden spectrum.

Dryden engineer Richard E. Maine implemented the state noise algorithm into the program, which was called MMLE. The program underwent various revisions, with the last being Version 3, or MMLE3.[27,28] Among other important contributions to the MMLE3 program, Maine is chiefly credited with adding significant programming efficiency, readability, and user friendliness to the code,

lending to its portability and early acceptance throughout the flight-test community.

The PID methods developed to extract aerodynamic coefficients were also applied to analyze structural dynamics—initially, with just simple aircraft vibrations. The DAST (drones for aerodynamic and structural testing) program afforded a unique opportunity to study a flutter-suppression vehicle.[21] Structural dynamics data from the DAST program were very useful primarily because of the high-sample-rate instrumentation onboard.

The Dryden PID technique was used on the space shuttle first during the unpowered approach and landing tests (ALT) in 1977, wherein the nonorbiting Shuttle *Enterprise* was released from a 747 carrier aircraft in flight. A close working relationship between Dryden's Iliff and Doug Cooke of NASA Johnson Space Center during the ALT flights led to subsequent Dryden PID support during operational space flights beginning in 1981. PID techniques developed at Dryden were adopted by NASA Johnson, the Air Force Flight Test Center, and shuttle prime contractor, Rockwell International. Analysts from each of the four organizations would independently analyze shuttle flight data (see following shuttle discussion) and then vote on what updates to make to the aerodynamic database to make the shuttle more viable in terms of safety and flight envelope availability.[29–31] shuttle data from Mach 27 down to Mach 0.3 were analyzed. In total, Dryden supported PID analysis of the orbiting shuttle for 17 years from 1981 through 1998. On some shuttle flights, structural dynamics was studied as well.

Between the late 1980s and mid-1990s, data from the X-29A and the F-18 were analyzed with the PID algorithm using state noise to model uncommanded forcing functions caused by separated and unsteady flows during flight at high angles of attack. More recently, various modified configurations of the SR-71 have been analyzed using PID to support envelope expansion and to study the effects of dynamic pressure and airframe flexibility on PID. These programs are discussed further in later sections of this paper.

Outside Dryden

It is generally accepted that modern parameter estimation techniques for aircraft had their origins at Dryden. Many of the principles behind system identification were developed almost 200 years ago by Gauss and advanced by others in the early 20th century. But the formalization, pulling together the theory and formulation from the ideas that Gauss and others had developed along with a method to solve the complete aircraft parameter estimation problem, was developed at Dryden. The number of MMLE programs distributed worldwide between the 1970s and mid-1980s reached the hundreds. Around 1985, Dryden engineers Richard E. Maine and James E. Murray developed an interactive version of the parameter estimation code called "pEst,"[32] which became the primary version for distribution from that point on. (The basic pEst program does not solve the nondeterministic state noise problem, but modifications can be made to enable it.) Even today, Dryden still receives questions and requests for the pEst program.

In the last 15–20 years, organizations other than Dryden have certainly advanced the basic techniques originally developed at Dryden. The organization with perhaps the greatest parameter estimation expertise in recent years, with the most people working on leading-edge parameter estimation problems, has been the DLR (German Aerospace Center) Institute of Flight Research in Braunschweig, Germany. Peter Hamel of DLR has long been one of the key international advocates for good parameter estimation as a keystone technology for flight testing, and Ravindra Jategaonkar has been one of the main contributors to the DLR expertise in this area.[33] Other notable researchers at DLR have included Juergen Kaletka, Ermin Plaetschke, and Susanne Weiss. The DLR and Dryden have worked together on PID dating back to at least 1970 and as recently as the mid-1990s during flight tests of the X-31 Enhanced Fighter Maneuverability demonstrator.[34] In the Netherlands, significant PID contributions have also been made by J. A. "Bob" Mulder at the Delft University of Technology and by Jan Breeman at the National Aerospace Laboratory.

During the 1980s, there was a resurgence of interest in PID analysis in the frequency domain. At NASA Langley, Vladislav Klein and Eugene A. Morelli conducted extensive research in this area,[35,36] (among other areas) which uses the same basic algorithms as in time-domain analysis, but with different modeling and constraints. (Prior to his tenure at Langley, Klein had already made important early contributions to the field while at Cranfield Institute of Technology in England.[37]) The work of Mark B. Tischler of the U.S. Army Aviation and Missile Command, Aeroflightdynamics Directorate at Moffett Field (NASA Ames Research Center), has been vital for helicopter and rotorcraft PID, again mostly in the frequency domain.[38] Although Dryden engineers had experimented with frequency-domain techniques in the 1960s, advantages of time-domain techniques proved more attractive.

The relative lack of commercialization of parameter estimation programs might in part be because Dryden in particular and others in general have given away their codes and provided technical assistance pro bono. In addition, the scarcity of new aircraft programs since the mid-1990s has limited the number of expert organizations to only government or university groups and a handful of private companies. Parts of the MMLE program have been modified for use in some commercial mathematical optimization programs.

Looking Back

The aircraft parameter estimation problem is one of the most successful applications of an engineering technique that relies heavily on a mathematical model to extract information from it. There have been four key contributors that have enabled the success of aircraft parameter estimation: 1) the mathematical model, which was established decades before; 2) high-quality vehicle and air data measurements, as the analysis would be no better than the data collected; 3) good maneuvers, provided either by a well-trained pilot or the control system; and 4) computational methods of analysis. The first three Ms were already in place by 1960. In some respects, it was pure happenstance that Dryden was in the right place at the right time with the right problem for digital computers to develop the fourth M. If Dryden had not done it, somebody else would have.

A partial list of aircraft at Dryden over the last 40 years that have utilized PID as a part of their flight-test program are shown in Table 1. Details of the programs and PID results from many of the programs can be found in technical papers available online on the Dryden Technical Report Server.* Dryden's level of PID participation varied from program to program, ranging from support roles in which PID was performed on a handful of maneuvers to lead roles in which PID was performed in support of full envelope expansion. To highlight some of these variations, the following remarks concerning the preceding aircraft are listed:

1) For aircraft 1, 22, 26–28, 32–39, 42, 47, 49, 50, 52, 54, 58, 60–62, and 64, PID was a major component of the flight-test program.

2) For aircraft 1, 2, 9, 17–20, 22, 23, 26–28, 32–39, 42–44, 47, 49–54, 58, 60–62, and 64, PID resulted in changes to the aerodynamic database and simulator and subsequently affected control system design and/or pilot training to address the issue identified by PID.

3) For aircraft 40, 41, 56, and 57, PID was under development during this program.

4) For aircraft 4, 5, 8, 10, 11, 13, 15, 16, 25, 30, 31, 45, 46, 48, 55, 59, 66, and 67, significant PID results were obtained, but program impact varied.

Methodology: the Maximum Likelihood Output-Error Approach

The basic concept of the maximum likelihood method is shown in Fig. 1. The measured vehicle response is compared with the estimated (simulated) response, and the difference between these responses is called the response error. A cost function includes this response error. A modified Newton–Raphson minimization algorithm is used to find the coefficient values (that is, the stability and control derivatives) that minimize the cost function. Each iteration of

*http://www.dfrc.nasa.gov/DTRS.

Table 1 Partial list of aircraft investigated at Dryden using PID

AD-1 Oblique-Wing Research Aircraft[a,b]	Firebee Drone and Drones for Aerodynamic and Structural Testing (DAST)[a,b]
B-1A[b]	Gossamer Albatross[a,b]
B-1B	Highly Maneuverable Aircraft Technology (HiMAT)[a,b]
B-2[d]	HL-10[a,b]
B-52[d]	Lockheed JetStar[a,b]
B-57B	M2-F1[c]
B-58	M2-F2[c]
Beech 99[d]	M2-F3[a,b]
Boeing 720[b]	NC-131H Total In-Flight Simulator[b]
Boeing 747[d]	Oblique-wing RPRV[b]
C-17[d]	PA30 [d]
C-47	Pegasus, Pegasus XL[d]
CV-990[d]	Space Shuttle Enterprise (tailcone on/off)[a,b]
DC-10	Space Shuttle launch stack[d]
F-4[d]	Space Shuttle Orbiter[a,b]
F-5[d]	Space Shuttle SCA [Shuttle Carrier Aircraft (modified 747)] with/without Orbiter[a,b]
F-8A Supercritical Wing[b]	SR-71[b]
F-8C Digital Fly-By-Wire[b]	SR-71 Test Bed with/without Linear Aerospike SR-71 Experiment (LASRE)[a,b]
F-14[b]	T-33 CalSpan Variable Stability Airplane[b]
F-15A[b]	T-37B[a,b]
F-15B	T-38[d]
F-15 3/8th-Scale remotely piloted research vehicle/ spin research vehicle (RPRV/SRV)[a,b]	X-15[c]
F-16[b]	X-15A-2 with/without external tanks[c]
F-16 Advanced Fighter Technology Integration (AFTI)	XB-70[a,b]
F-16 XL[d]	XV-15 Tiltrotor Research Aircraft[d]
F-18[a,b]	X-24A[a,b]
F-18 High Alpha Research Vehicle[a,b]	X-24B[a,b]
F-18B Systems Research Aircraft[a,b]	X-29A[a,b]
F-100	X-31
F-102[d]	X-38[a,b]
F-104[d]	YF-12A
F-111A[a,b]	YF-16[d]
F-111 AFTI[a,b]	YF-17[d]
F-111 Transonic Aircraft Technology[a,b]	YT-2B

[a]PID was a major component of the flight test program.
[b]PID resulted in changes to the aerodynamic database and simulator and subsequently affected control system design and/or pilot training to address the issue identified by PID.
[c]PID was under development during this program.
[d]Significant PID results were obtained but program impact varied.

this algorithm provides a new estimate of the unknown coefficients on the basis of the response error. These new estimates are then used to update values of the coefficients of the mathematical model, providing a new estimated response and, therefore, a new response error. Updating of the mathematical model continues iteratively until a convergence criterion is satisfied. The estimates resulting from this procedure are the maximum-likelihood estimates.

The maximum-likelihood estimator also provides a measure of the reliability of each estimate based on the information obtained from each dynamic maneuver. This measure of the reliability, analogous to the standard deviation, is called the Cramér–Rao bound.[11,39,40] The Cramér–Rao bound, as computed by current programs, is better understood as a measure of relative, rather than absolute, accuracy. Moreover, it is often useful to multiply the Cramér–Rao bound by an integer factor to provide an "uncertainty level" of the computed estimates. This factor is selected by engineering judgment based on the number of variables unaccounted for in the derivative plot (such as control surface position, maneuver amplitude, Mach number, dynamic pressure, and altitude), the number of maneuvers at a specific flight condition, and the quality of the instrumentation system. A rigorous treatment of the Cramér–Rao bound and the use of multiplying factors is given in Ref. 39. In the derivative plots to follow, the aforementioned uncertainty levels are denoted as vertical bars.

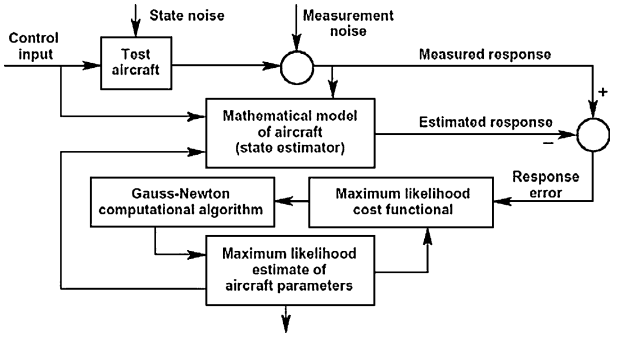

Fig. 1 Maximum likelihood estimation concept with state and measurement noise.

Fig. 2 X-29A aircraft, number 2.

A precise, mathematically probabilistic statement of the parameter estimation problem and the formulation of the maximum-likelihood output-error approach (with and without state noise) have been described in detail in several publications[40–43] and are not repeated herein. Practical lessons learned from a wide variety of PID applications have also been published.[44–47] Reference 48 presents a comprehensive bibliography of over 400 books, papers, and reports through 1986 related to aircraft parameter estimation. The remainder of this paper discusses several applications of the present technique during the last 12 years at Dryden.

Recent Examples

The following examples of parameter estimation over the past 12 years at NASA Dryden all utilized the Dryden-developed pEst code.[32] Some program modifications were necessary to account for state noise, and such cases are pointed out in the respective applications. Four flight vehicles are discussed: the X-29A,[49] the F-18,[22,23,50] the SR-71,[51,52] and the space shuttle.[31] A brief introduction to each of the vehicle programs is followed by select, though typical, PID results from the flight program. A complete set of analyzed derivatives and program details can be found in the associated references.

X-29A

The X-29A Advanced Technology Demonstrator program was conducted between 1984 and 1992 at NASA Dryden to explore transonic aerodynamics, composite aerostructures, airfoil technology, flight dynamics, and stability and control. Two aircraft were built by the former Grumman Aerospace Corporation under sponsorship by the Defense Advanced Research Projects Agency (DARPA) and funded by the U.S. Air Force. The prime research objective was to test the predicted aerodynamic advantages of the unique forward-swept-wing (FSW) configuration and its unprecedented level of static instability for an airplane.

Figure 2 shows a flight photo of the second X-29A aircraft. The three-surface pitch control uses close-coupled, variable incidence

canards, the full-span wing flaperon, and small strake flaps at the rear of the aircraft. Operated differentially, the full-span, double-hinged, variable camber flaperons also provide lateral control. These flaperons provide all roll control, as the configuration does not use spoilers, rolling tail, or differential canards. A conventional rudder mounted on a fixed vertical stabilizer provides directional control. Whereas the aircraft is statically stable in the lateral-directional axes, the aircraft is statically unstable in the longitudinal axis, with a negative static margin of up to 35% at subsonic speeds. Reference 47 includes an analysis of X-29A longitudinal maneuvers at unstable flight conditions. In the supersonic regime approaching Mach 1.4, the aircraft exhibits near-neutral stability. For accurate flight-path targeting, an uplink system was employed to help the pilot capture and hold precise test points, especially during maneuvers at high angles of attack (AOA). This uplink targeting system proved useful for the stability and control PID maneuvers discussed in Ref. 49.

During flights 6 to 30 from October 1989 to March 1990 and flights 117, 118, and 120 in September 1991, a total of 52 lateral-directional maneuvers were performed using pilot-input doublets to provide data for analysis with the pEst program. All 52 maneuvers were performed at subsonic, 1-g flight conditions. Maneuvers performed above 15-deg AOA were analyzed using state noise to model uncommanded motions resulting from unsteady aerodynamics (separated and vortical flows) over the aircraft. Analysis of this data was a challenge because of difficulties in holding the flight condition, especially at high AOA, and the inability to separate aileron and rudder effects caused by the flight control system (see the following).

This analysis supported the high-AOA envelope expansion phase of the second X-29A by providing flight-determined values of the aircraft's lateral-directional stability and control derivatives. The derivatives were used to update the aeromodel, improve the real-time simulator, and revise flight control system laws. The results were also used to evaluate preliminary design and prediction techniques used to develop the aircraft (e.g., computational-fluid-dynamics and structural-dynamics simulations).

One of the main difficulties in PID analysis was caused by the high-gain feedback control system of the X-29A. For example, the aileron-to-rudder interconnect resulted in rudder motions not caused by rudder pedal input but by aileron stick input. The effect of this interconnect over large portions of the maneuver hampered the separation of aileron effect from the rudder and rate effects. The control system also contributed to smaller maneuver excursions, artificially highly damped responses, and high correlation between the responses and control motions, resulting in very little independence between the control derivatives and the damping derivatives. To address this near-derivative dependence, a small a priori weighting[11] based on analytical predictions was used on the damping derivatives.

A full suite of lateral-directional stability and control derivatives was extracted from the 52 maneuvers and presented in Ref. 49. Two of these derivatives are presented herein. Each derivative is plotted as a function of AOA, where the circle symbols are the flight estimates, the vertical lines are the uncertainty levels, and the dashed line is the fairing of predicted values from the wind-tunnel-derived AERO9B simulation database. The uncertainty levels[39,44] shown on the plots as vertical bars are obtained by multiplying the Cramér–Rao bound of each estimate by a factor of three. The solid fairing is the authors' interpretation of the flight data over the entire AOA range, based on uncertainty levels, the scatter of adjacent estimates around a given AOA, and engineering judgment of the maneuver quality. Theoretically, information on maneuver quality such as the length of the maneuver, amount of control input, excitation of the response variables (sideslip, roll rate, yaw rate, and lateral acceleration), and correlation between control motions is contained in the value of the uncertainty level. A large uncertainty level indicates low information on the derivative estimate for that maneuver, and a small uncertainty level indicates high information.

Figure 3 shows predicted (dashed line) and flight-determined (circle symbols and solid line) Cl_β (dihedral) for the X-29A. The solid line denotes the flight fairing, and the vertical bars represent the uncertainty levels for each estimate as defined earlier. The agreement between the predicted and flight-determined dihedral is good below 7-deg AOA. The flight data show more scatter and larger uncertainty levels above 18-deg AOA with values varying between -0.002 and -0.004 and the predominant trend showing a value of about -0.003. The predicted data show Cl_β decreasing to around -0.006 at 20-deg AOA and then approaching the flight values at 42 deg before once again decreasing to -0.005 above 45 deg. This is a significant disagreement between prediction and flight above 20-deg AOA in this very important derivative. A primary effect of Cl_β is its contribution to the static directional stability of the vehicle. The flight responses show that the vehicle is somewhat less statically stable at high AOA than the original prediction, which is apparent with the flight estimates being less negative (smaller in magnitude) than the predictions.

The difference between flight and prediction is significant, but this might be partly because the flight maneuvers were performed at somewhat larger sideslip angles than those used to calculate the predicted values. The predicted wind-tunnel value of Cl is a nonlinear function of β and, therefore, depends on the amount of β over which the derivative is linearized. In addition, the predicted value of Cl_β shows a dependence on the position settings of the three pairs of longitudinal control surfaces (canards, flaperons, and strakes), which vary in flight with AOA. Reynolds-number effects are also known to cause differences between wind-tunnel predictions and flight results, especially where vortex flows are dominant. The Reynolds numbers for the flight data examined here are between 5×10^6 and 6×10^6 and are nearly an order of magnitude larger than the Reynolds numbers for most of the wind-tunnel tests. The sawtooth appearance of the prediction fairing, evident in Fig. 3, is not so much a function of the plotted abscissa (AOA) as it is of the aforementioned differences between flight and prediction concerning angle of sideslip and longitudinal control surface position.

Figure 4 shows the aileron effectiveness $Cl_{\delta a}$ as a function of AOA. The decreasing trend of the predicted (dashed) and flight-determined (solid) $Cl_{\delta a}$ is similar below 25-deg AOA, with the flight estimates being lower by up to 0.0005. Above 30-deg AOA, the predicted value is about half of that determined from flight. The flight-determined roll control power is fairly good all of the way to 53 deg, which is unusual for conventional, aft-swept wings. This good effectiveness could result from a combination of the FSW and the strong flow off the canard that is just ahead of the wing. This resulting effectiveness provides the pilot enhanced ability to hold a bank angle at extreme AOA and improved closed-loop damping-in-roll caused by the high-gain control system working through the good control effectiveness. The increased aileron roll control at high AOA is achievable because the typical stall pattern of an aft-swept wing, from wing tip to root, is reversed for a FSW, which stalls from root to tip.

Reference 49 includes other interesting findings such as the detection of suspected asymmetric vortex switching over the F-5A nose section of the X-29A at high angles of attack, as evident in the

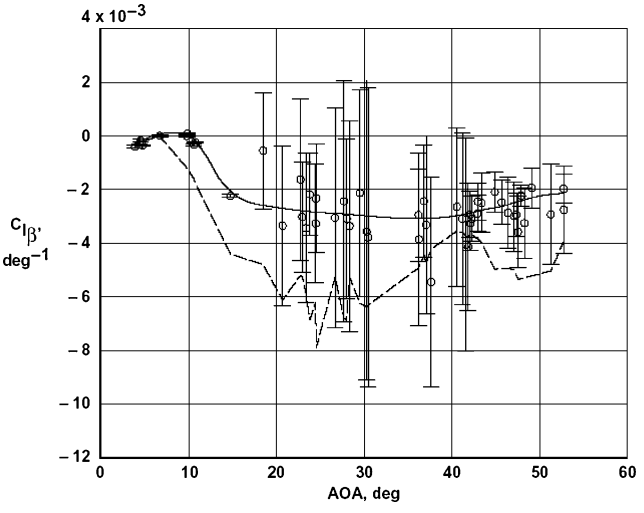

Fig. 3 X-29A Cl_β as a function of AOA.

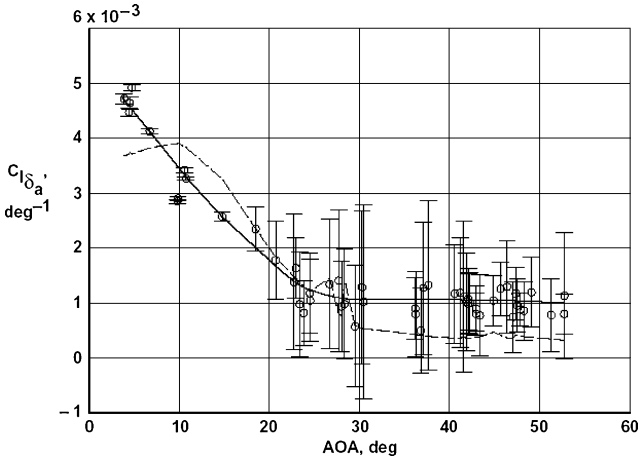

Fig. 4 X-29A $Cl_{\delta a}$ as a function of AOA.

Fig. 5 F-18 high-Angle-of-Attack research vehicle.

bias coefficients of rolling and yawing moment. Also, flight values of rudder effectiveness were found to be larger than prediction.

F-18 High Angle of Attack Research Vechicle

The High Angle of Attack Technology Program (HATP) was a multiyear program that began in the mid-1980s and spanned over a decade to investigate flight at high AOA. The aircraft used in the flight portion of the HATP was an F/A-18 that was subsequently named the F-18 High Angle of Attack Research Vehicle (HARV). The F/A-18 is a single-seat aircraft that features a midwing configuration with a wing-body strake—or wing-root leading-edge extension (LEX)—that extends from the forward portion of the fuselage and blends into the wing. Previously used for high AOA and spin testing by the U.S. Navy, the F-18 HARV conducted its first NASA research flight on 2 April 1987 and its final research flight on 15 May 1996, 388 research flights later.

Phase I of the HARV program involved the basic F-18 configuration and spanned from 1987 to 1989. During this period, the HARV investigated high-AOA aerodynamics and handling characteristics to a maximum of 55-deg AOA. Phase I PID activities evaluated stability and control derivatives obtained from wind-tunnel tests and early flight tests by the manufacturer and U.S. Navy.[50,53]

Phase II involved major hardware and software modifications to the HARV. A multi-axis thrust-vectoring control system (TVCS) consisting of externally mounted nozzle postexit vanes was added to the aircraft (see Fig. 5), as well as a specialized research flight control system (RFCS). The design was intended for research purposes only and not for production. Phase II flight testing spanned from mid-1991 to late 1994. Demonstrated capabilities included stabilized flight at 70-deg AOA and rolling at high rates at 65-deg AOA. The configuration studied during phase II also included the LEX fence modification introduced in early 1989 to reduce vertical tail buffet caused by impingement of the LEX vortex. Figure 6 shows an aft view of the phase II HARV with TVCS hardware. The third and final phase between 1995 and 1996 investigated the use

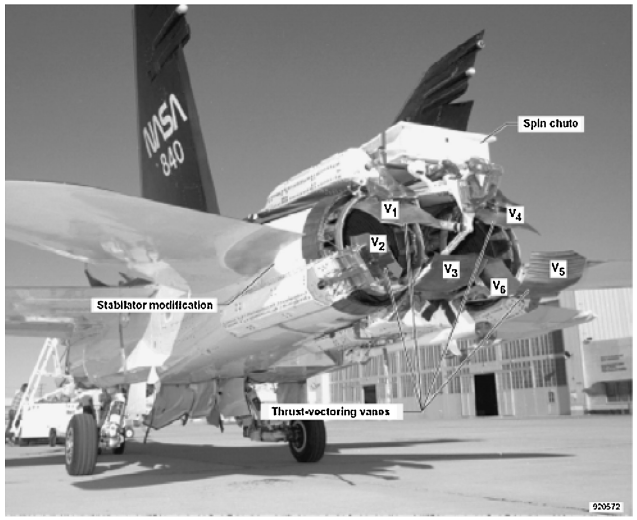

Fig. 6 Thrust-vectoring control system hardware.

of conformal forebody strakes on the nose of the HARV to enhance lateral-directional control at high AOA.

The aircraft was extensively instrumented for research purposes. The sensor suite included three-axis linear accelerometers, attitude and angular-rate gyros, control surface position transducers, and redundant air-data sensors. Air data were measured or derived from multiple sources including production air-data sensors mounted on the forward fuselage, the inertial navigation system, swiveling (self-aligning) pitot probes mounted on both wing tips, and a pneumatic flush air-data system located on the nose cone. During phase I flights up through Flight 38, the HARV was also outfitted with a standard NACA noseboom-mounted probe to calibrate the wing-tip probes. Other instrumentation included thermocouples and strain gauges to measure temperatures and loads on the thrust-vectoring vanes, video cameras for flow-visualization studies, and sensors to monitor engine thrust and fuel consumption (from which instantaneous mass and inertia characteristics could be calculated).

As required for proper PID analysis, measurements of AOA and sideslip were corrected for c.g. offset. Corrections for upwash, sidewash, and boom-bending effects were also made for boom-obtained air data. Linear accelerometer data were corrected in the PID program for instrument offsets from the c.g. Furthermore, before the maneuvers were analyzed, the data were corrected for time lags introduced by sensor dynamics and signal filtering. Making these corrections is critical to adequately estimate stability and control derivatives.[44]

Although several organizations performed PID analysis of the HARV, the present examples focus exclusively on efforts by the present authors.[22,23,50] The examples cover PID flights during phase I and phase II. The maneuvers were analyzed with the pEst computer program with state noise modifications in order to account for uncommanded responses in the separated flow regime encountered at high AOA. All maneuvers were subsonic and performed as small perturbation maneuvers about the 1-g flight condition at a given AOA. Uncertainty levels were obtained by multiplying the Cramér–Rao bound of each estimate by a factor of five.

Phase I HARV

PID analysis of the basic F-18 HARV during phase I flights revealed two main difficulties related to the maneuvers and their analysis, both of which were similarly experienced during flight testing of the X-29A. The first issue was one of aerodynamics, resulting from unsteady separated and vortical flows over the aircraft above 20-deg AOA, which caused the aircraft to exhibit uncommanded motions of varying amplitude and frequency. (A good discussion of maneuver difficulties and related analysis issues under high-AOA flight conditions is found in Ref. 24 for the 3/8-scale F-15 Remotely Piloted Research Vehicle.) The effect of the uncommanded forcing functions was accounted for by considering state noise in the

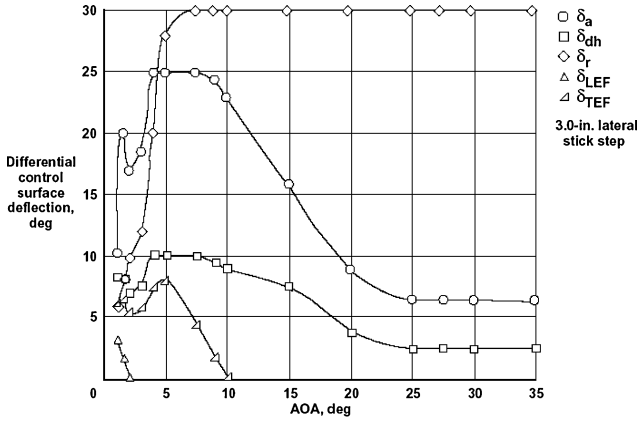

Fig. 7 Differential control surface deflection schedule caused by aileron input (with ARI).

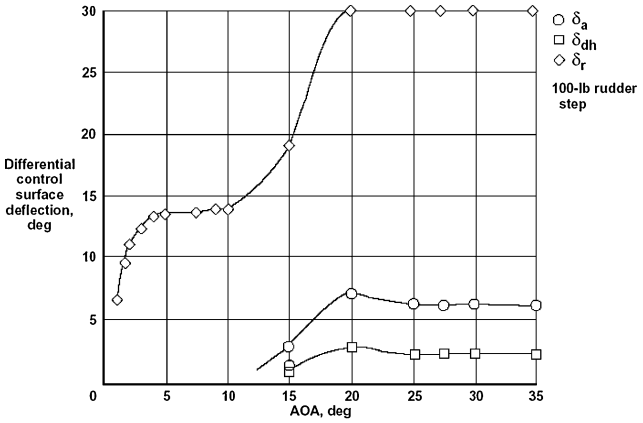

Fig. 8 Differential control surface deflection schedule caused by rudder input (with RAI).

modeling. State noise was assumed for all PID maneuvers on the phase I HARV regardless of AOA, although the uncommanded responses were only significant above 20-deg AOA.

The other difficulty arose because the maneuvers were performed with the basic F-18 control system engaged. The maneuvers were less than ideal for derivative extraction because of near linearly dependent[44] motions of the controls (especially above 25-deg AOA) and relatively high correlations between the response variables and the resulting control motions caused by the feedback control system. These correlations were further complicated because their interrelationships were functions of angle of attack. This situation made it difficult to obtain good independent estimates of individual controls as well as estimates for an equivalent control derivative—that is, a combination of two or more controls. Figures 7 and 8 illustrate the multisurface control deflection schedule as a result of aileron and rudder input, respectively; deflections are shown for aileron δ_a, differential horizontal stabilator δ_{dh}, rudder δ_r, and asymmetric leading-edge flap δ_{LEF}, and trailing-edge flap δ_{TEF}. The effects of the aileron-to-rudder interconnect (ARI) and rudder-to-aileron interconnect (RAI) are evident.

Above 15-deg AOA, the linear correlation between the two controls, aileron δ_a and differential horizontal tail δ_{dh}, is approximately 0.42. Because of poor estimates of the individual controls, an equivalent combined lateral control δ_L is used to capture their combined effectiveness. Thus, above 15-deg AOA, the coefficients of rolling moment, yawing moment, and lateral force as a result of lateral control are, respectively,

$$Cl_{\delta L} = Cl_{\delta a} + 0.42Cl_{\delta \text{dh}} \tag{1}$$

$$Cn_{\delta L} = Cn_{\delta a} + 0.42Cn_{\delta \text{dh}} \tag{2}$$

$$CY_{\delta L} = CY_{\delta a} + 0.42CY_{\delta \text{dh}} \tag{3}$$

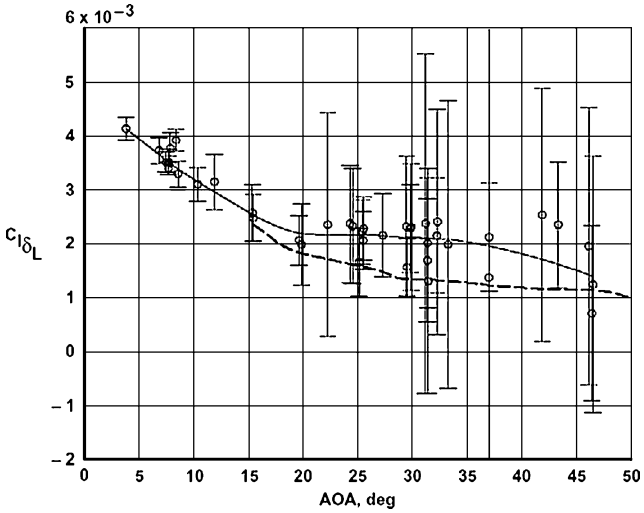

Fig. 9 F-18 equivalent lateral control derivative as a function of AOA.

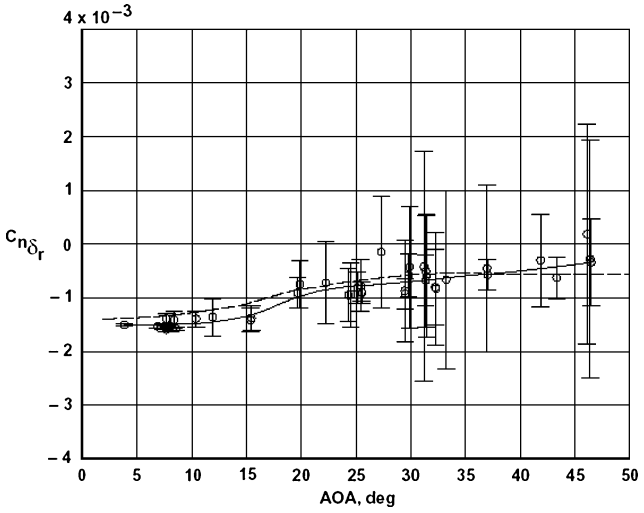

Fig. 10 F-18 rudder effectiveness as a function of AOA.

Wind-tunnel predictions of $Cl_{\delta L}$, $Cn_{\delta L}$, and $CY_{\delta L}$, used for comparison with flight-estimated values, are calculated with the same preceding equations.

Figure 9 shows flight estimates (solid line) and wind-tunnel predictions (dashed line) for the derivative of rolling moment as a result of equivalent combined lateral control $Cl_{\delta L}$ as a function of AOA. Above 15-deg AOA, both extracted and predicted lateral control derivatives are as defined earlier. Below 15-deg AOA, flight estimates and fairings are given, but wind-tunnel predictions are not assumed in this range because of the more complicated control surface dependencies as evident in Fig. 7. The trend of the lateral control effectiveness $Cl_{\delta L}$ for both flight estimates and wind-tunnel predictions is more or less the same. The agreement varies, with the flight estimate showing 10 to 30% more effectiveness. Although the derivative is plotted as a function of AOA, other variables, such as altitude (and thus Reynolds number) and horizontal stabilator position, account for some of the scatter in the flight estimates.

Despite the effect of the RAI on rudder input (Fig. 8), the rate limit in the δ_r surface results in some linear independence between δ_a and δ_r, which allows the rudder derivatives to be estimated independent of the equivalent lateral control variable δ_L. Figure 10 shows rudder effectiveness $Cn_{\delta r}$ as a function of AOA, with good agreement throughout the AOA range, but the flight values (solid) indicate somewhat more effectiveness below 35-deg AOA than the predicted values (dashed).

Phase II HARV

PID maneuvers during HARV phase II flight testing were also analyzed using the pEst program with state noise present to account for uncommanded motions caused by unsteady flow phenomena at high AOA. All phase II maneuvers (25 longitudinal and 26 lateral directional) were subsonic and performed as small perturbation maneuvers about the 1-g flight condition at AOAs of approximately 10, 20, 30, 40, 50, 60° (longitudinal and lateral directional), and 70 deg (lateral-directional only). Unlike phase I maneuvers, however, phase II maneuvers were not performed by a pilot but by a unique research tool called the onboard excitation system (OBES) while the vehicle was under the control of the RFCS.

Software within the OBES held preprogrammed research and envelope expansion maneuvers that were used for flutter envelope clearance, control power research, and aerodynamic and control law PID. For PID, the OBES, when activated by the pilot, would command single-surface inputs (SSIs) through the RFCS to particular control surfaces. By permitting single-surface aerodynamic control deflections, control surface correlation problems were eliminated from the PID analysis—in contrast to the analysis of the basic F-18 just discussed. Independent thrust-vectoring vane deflections were also available with the OBES; these deflections were not single-vane but rather single-axis deflections, using all vanes to excite responses in either the pitch or yaw axis. As Fig. 6 shows, V_1, V_2, and V_3 are the upper, outer, and inner vane deflections for the left engine; and V_4, V_5, and V_6 are the upper, outer, and inner vane deflections for the right engine. If the vanes are assumed to be touching the exhaust plume, the equivalent pitch vane and yaw vane inputs are defined by the following equations:

$$\delta_{\text{pv}} = \{[V_1 - (V_2 + V_3)/2 + V_4 - (V_6 + V_5)/2]/2\}T \qquad (4)$$

$$\delta_{\text{yv}} = \{[(V_2 - V_3)/2 + (V_6 - V_5)/2]/2\}T \qquad (5)$$

where T is equal to $T_L + T_R$, the combined thrust of both left and right engines.

Phase II HARV Longitudinal

A total of 25 longitudinal stability and control maneuvers were performed using the OBES. The maneuvers were performed in AOA increments of 10 deg, resulting in six maneuver "groups" at approximately 10 deg (five maneuvers), 20 deg (three maneuvers), 30 deg (five maneuvers), 40 deg (five maneuvers), 50 deg (four maneuvers), and 60 deg (three maneuvers) AOA.

Ideally, all maneuvers of a given control surface should be performed with the same input amplitude within the same AOA group and preferably across all AOA groups, too. Unfortunately, this was not the case. For example, all of the maneuvers at 20- and 30-deg AOA had amplitudes of elevator doublet and symmetric aileron doublet that were 70% greater than those in the other AOA groups.[22] In addition, there were similar variations in control input amplitude between maneuvers within the same AOA group. Some large-amplitude inputs resulted in such large AOA excursions that they violated the small-perturbation assumptions used to linearize the equations of motion, such that truncation of the maneuver was necessary prior to analysis. These undesirable variations in amplitude of the OBES doublets made the interpretation of PID results somewhat cumbersome. Nevertheless, each maneuver itself was excellent in that sufficient response was obtained from the substantially independent control doublets.

Flight-extracted derivatives are plotted as functions of AOA, wherein the dashed lines represent predicted values taken from subscale, cold-jet ground tests[54] and a simulation based primarily on wind-tunnel data of the basic F-18 configuration[55,56] without the LEX fence and TVCS airframe modifications. Although the derivatives are plotted as functions of AOA, other variables (such as altitude, Reynolds number, Mach number, and horizontal stabilator position) account for some of the data scatter seen in the plotted estimates.

Figure 11 shows the coefficient of normal force caused by trailing-edge flap (TEF) as a function of AOA. The flight values are lower

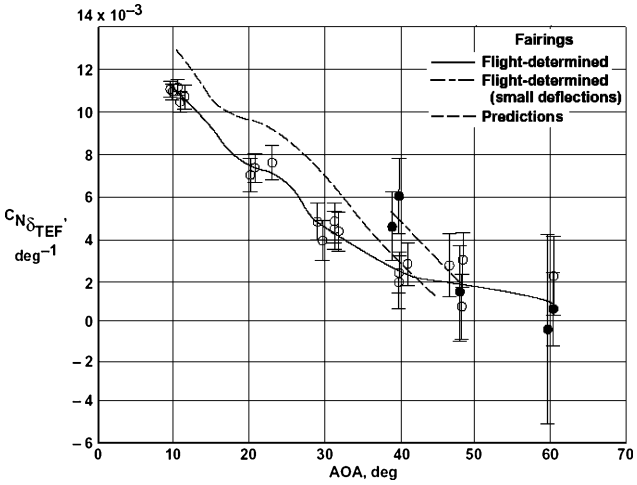

Fig. 11 F-18 HARV normal force as a result of TEF as a function of AOA.

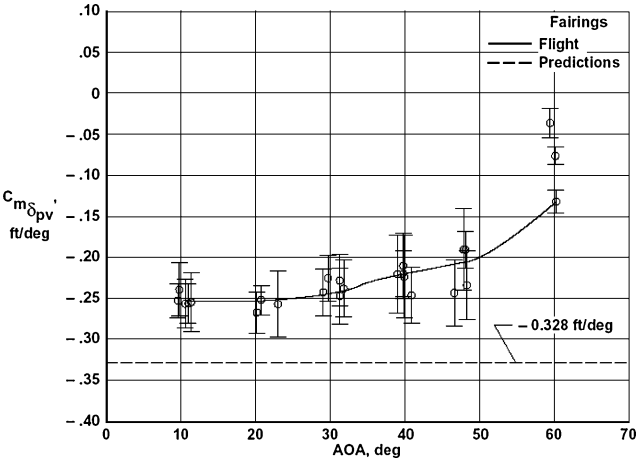

Fig. 12 F-18 HARV pitch vane effectiveness derivative as a function of AOA.

than predicted below 42-deg AOA. The shaded symbols indicate maneuvers with smaller-amplitude δ_{TEF} doublets. In particular, two of these maneuvers are near 40-deg AOA and a third near 50-deg AOA, through which a secondary fairing (dashed) is drawn. The secondary fairing suggests somewhat more normal force per degree of deflection for small deflections than for large deflections, attributable to nonlinearities in control surface effectiveness as a function of deflection amplitude. Perhaps the same would be true at other AOAs, but no evaluation can be made because the δ_{TEF} doublets at 10-, 20-, and 30-deg AOA are either all large or all small. Reference 22 reports that larger force and moment coefficients are also seen with elevator doublets with smaller-amplitude deflections than those with larger-amplitude deflections (though this is not the case with the symmetric aileron doublets).

TVCS vane derivatives are different than typical aerodynamic control derivatives as they are not strictly functions of flight condition such as velocity or dynamic pressure. Thus, vane derivatives are normalized by dividing the moment (ft-lb) and force (lbf) by both the thrust and the vane deflection [Eqs. (4) and (5)], resulting in units of feet/degree for moment coefficients and deg−1 for force coefficients. Figure 12 shows the flight-determined values of $Cm_{\delta\text{pv}}$ to be about −0.25 ft/deg up to 30-deg AOA, with gradually decreasing magnitudes at higher AOA. Poor agreement is seen with the prediction of −0.328 ft/deg. The reason for this decreased effectiveness is found by plotting individual vane deflection on top of the (least-squares fit of the) normalized load on that vane. Reference 22 shows that the deflection of a single vane affects the load on the opposing vane or vanes. The unanticipated impingement of the vectored plume on the opposing vane or vanes results in reduced vane

effectiveness, an effect called plume pinching.[22] Thus, for the large 5-deg deflections of the δ_{pv} doublet, a 1- to 1.5-deg apparent" deflection on the opposing vanes would result in a 20 to 30% reduction in pitch vane effectiveness.

The potential 20 to 30% reduction in effectiveness is about that seen in Fig. 12 for $Cm_{\delta pv}$ between 10- and 30-deg AOA. The reduced effectiveness above 30-deg AOA can be caused by additional effects of the free airstream. The much-reduced effectiveness at 60-deg AOA can result from the exact point of contact between the vane and the plume being more difficult to identify. Also, because the stabilator is saturated for trimmed flight above 55-deg AOA a nonzero steady-state δ_{pv} is required to maintain 60-deg AOA flight. Thus, the actual δ_{pv} doublet is commanded in addition to this nonzero pitch vane input. Taking into consideration the preceding discussion, the agreement between flight-determined and predicted values of $Cm_{\delta pv}$ is very good up to 30-deg AOA and fairly good at 40- and 50-deg AOA.

Phase II HARV Lateral Directional

A total of 26 phase II lateral-directional PID maneuvers were performed using the OBES. The maneuvers were performed in AOA increments of 10 deg, resulting in seven maneuver groups at approximately 10 deg (five maneuvers), 20 deg (five maneuvers), 30 deg (five maneuvers), 40 deg (four maneuvers), 50 deg (three maneuvers), 60 deg (three maneuvers), and 70 deg (one maneuver) AOA. Each of the four lateral-directional control surfaces (differential stabilator deflection δ_{dh}; rudder deflection δ_r; aileron deflection δ_a; and equivalent yaw vane deflection δ_{yv}) was independently commanded using a distinct 4-s doublet approximating one full cycle of a square wave. (Although the OBES input commands were for a pure doublet, the actual control deflections were not perfect square waves as a result of some modification by the RFCS. Nevertheless, these SSIs are far superior to those for the basic F-18.) Although the OBES allowed for consistent and repeatable maneuvers, there were a few maneuvers with different control input amplitudes (and resultant dynamic response)—as occurred with the longitudinal maneuvers. These cases correspond to maneuvers 10, 12, 16, and 20, which were flown on the first HARV phase II PID flight (flight 155). In some of the figures to follow, these early maneuvers are highlighted with flagged solid symbols.

Figure 13 shows the dihedral sideslip derivative Cl_β as a function of AOA. The agreement of flight-determined (solid) Cl_β with prediction (dashed) is good below 20-deg AOA and at 50-deg AOA. The estimates for the flight data are tightly clustered at most AOAs and have relatively small uncertainty levels, providing a fairly high confidence in the flight values. Disagreement with predicted values might be caused by differences in flight condition between flight estimates and predictions. Flight values of Cl_β were determined over a $\Delta\beta$ peak-to-peak range of 10. Because the β derivatives are usually

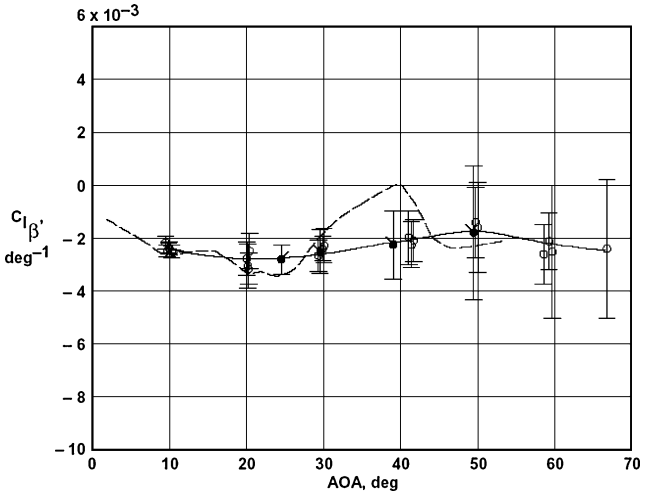

Fig. 13 F-18 HARV sideslip derivative (dihedral) as a function of AOA.

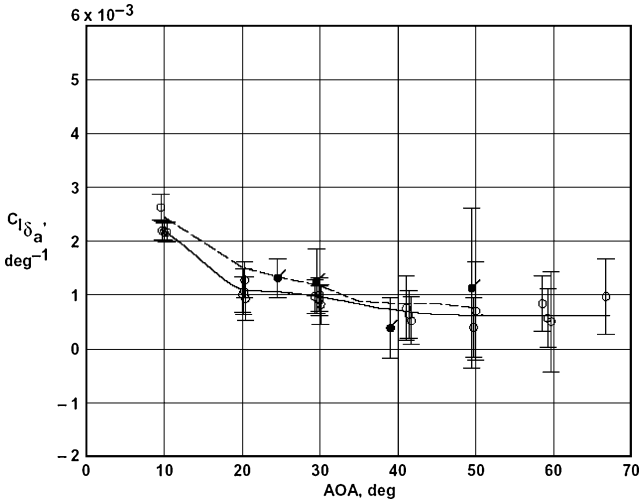

Fig. 14 F-18 HARV aileron derivative as a function of AOA.

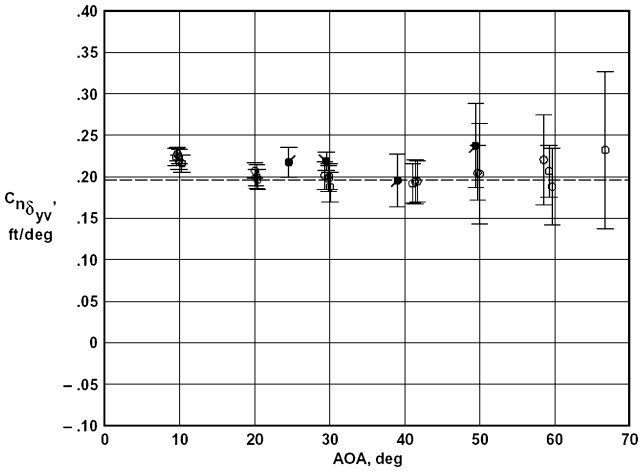

Fig. 15 F-18 HARV yaw vane effectiveness derivative as a function of AOA.

nonlinear with sideslip angle, the range of sideslip over which the derivatives are defined makes a difference. The sideslip range for the predictions is likely smaller than the flight range $\Delta\beta$. In addition to differences in sideslip range, the LEX fences installed on the HARV would certainly be expected to affect Cl_β (especially in the AOA region greater than 25 deg dominated by strong vortical flow), a factor not accounted for in the predictions.

Figure 14 shows the comparison of the flight (solid) and predicted (dashed) values for $Cl_{\delta a}$, a derivative that could not be obtained for the basic F-18 because of close correlations between aileron and rudder controls. The flight value is 10 to 25% lower than predicted throughout the AOA range. The flight estimates are seen to be good, especially for high AOA, as the estimates are tightly clustered with relatively small uncertainty levels at less than 50-deg AOA. At approximately 10-deg AOA, the flight maneuvers have $\Delta\delta a$ amplitudes of approximately ± 5 deg, and elsewhere the maneuvers have $\Delta\delta a$ amplitudes of approximately ± 11 deg, except for the four flagged solid symbols. The four flagged values correspond to $\Delta\delta a$ amplitudes of approximately ± 8 deg. The two flagged solid symbols at 25- and 30-deg AOA are in good agreement with the prediction, which might indicate that the prediction is based on a $\Delta\delta a$ range smaller than the ± 11-deg range of the other maneuvers.

Figure 15 shows the comparison of flight and predicted (dashed) values of $Cn_{\delta yv}$ as a function of AOA. The flight estimates are slightly higher than predicted for AOAs less than 30 deg and are in good agreement elsewhere. The flagged solid symbols indicate the four maneuvers from the first flight where the variation in vane deflection $\Delta\delta_{yv}$ was ± 10 deg, in contrast to the other maneuvers at 20-deg AOA

and greater in which the variation was ±18 deg. All four of these flagged flight estimates show the highest values of $Cn_{\delta yv}$ for their AOA range and therefore indicate that vane effectiveness might be somewhat higher for small δ_{yv} deflections than for large deflections, which is consistent with findings in Ref. 54. Moreover, the five flight estimates grouped at approximately 10-deg AOA, in which the $\Delta\delta_{yv}$ was only ±10 deg, clearly show a higher estimate than predicted. Because the prediction represents the ideal case (in terms of plume-to-vane deflection ratio) where the vane effectiveness is at a maximum, the most likely explanation for the difference in prediction and flight is that the thrust calculation used to define δ_{yv} for $\Delta\delta_{yv} = \pm 10$ deg is at least 10% too high. Further supporting this conclusion, Ref. 22 also shows flight estimates of $CN_{\delta pv}$ to be 10% higher for small vane deflections at low AOA than their ideal values (where no plume pinching occurred).

Reference 23 compares flight-determined derivatives from phase I with derivatives from phase II (where applicable). As expected, phase II derivatives are superior to phase I derivatives as evidenced by tighter clustering of estimates and smaller uncertainty levels; this is a direct result of the excellent quality and near repeatability of the automated OBES maneuvers compared to manual pilots inputs. Looking back on the OBES maneuvers, it is clear that 10-deg AOA increments (between maneuver groups) were too large to adequately define the derivatives as functions of AOA. Derivative variations can occur over AOA increments as small as 2 or 3 deg, although increments of 5-deg AOA would probably have been sufficient. Better characterization of the derivatives in terms of variable or control deflection range (i.e., doublet size) could also have been achieved by better maneuver design using the OBES.

Following the conclusion of the HATP in 1996, the wings from the F-18 HARV airframe were subsequently removed, modified, and installed on another F-18 to support NASA's Active Aeroelastic Wing (AAW) program currently at Dryden. In anticipation of conducting PID studies on the AAW vehicle in the near future, a recent NASA paper[57] by Dryden engineer Timothy R. Moes et. al. discusses the analysis of an F-18B flying at high dynamic pressures to investigate the effects of airframe flexibility on PID derivative extraction.

SR-71

The SR-71A is a two-place, twin-engine aircraft capable of cruising at speeds up to Mach 3.2 and altitudes up to 85,000 ft. Following retirement of the fleet from operational status in 1990, three SR-71s were loaned to NASA from the USAF for use as high-speed research platforms. Between 1997 and 2001, a number of maneuvers were performed on the SR-71A to facilitate aerodynamic PID of the baseline SR-71A and two modified configurations of the SR-71A. The first modification was in support of the X-33 Linear Aerospace SR-71 Experiment (LASRE). This configuration, shown in Fig. 16, involved the addition of internal and external hardware to the upper aft fuselage to enable flight tests of the unique linear aerospike rocket engine installed in a subscale, half-span model of the X-33 lifting body. The model was mounted on a reflection plane to isolate the aerodynamics between the aircraft and model and supported via structural stand-off fixtures known as the "canoe" and "kayak." The model was vertically oriented so that angle of sideslip excursions of the SR-71A imparted angle-of-attack excursions on the model. The second modified configuration consisted of only the reflection plane, canoe, and kayak; without the X-33 model, this was known generically as the test-bed configuration (Fig. 17), because it could theoretically support experiments other than just the LASRE.

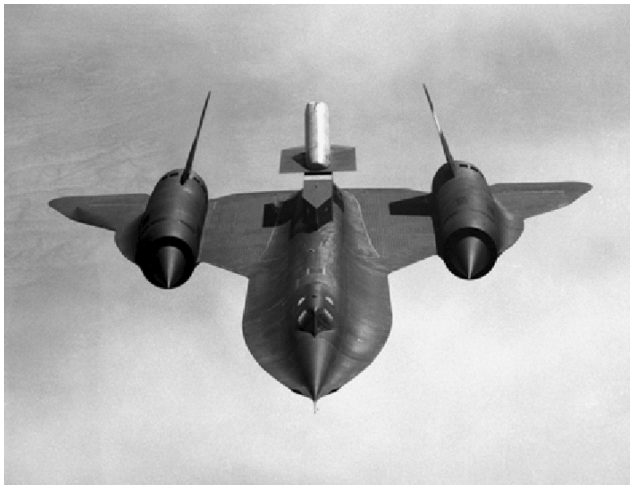

Fig. 16 SR-71 LASRE configuration.

Fig. 17 SR-71 test-bed configuration.

Because of the large size of the LASRE and test-bed configurations, an incremental stability and control flight envelope expansion was necessary to ensure safe flying characteristics. PID maneuvers included pilot-input doublets across a range of Mach numbers. The LASRE configuration obtained flight data at speeds up to a maximum of Mach 1.75. The test bed configuration flight program was conducted up to a maximum speed of Mach 3.0. Both pitch doublets and yaw-roll doublets were performed to extract longitudinal and lateral-directional derivatives, respectively. Results from the baseline SR-71A were compared to predicted values from the basic SR-71 aerodynamic model. Data were also obtained at low and high equivalent airspeeds to determine the effect of aircraft flexibility on the stability and control derivatives.

Although results from the PID analysis are not presented herein (please see Refs. 51 and 52), the recent SR-71 experience at Dryden is mentioned herein, however briefly, as yet another example of the classic role of PID in safely expanding the flight envelope within the context of a step-by-step flight-test program in which new vehicle configurations are evaluated in terms of their effect on handling qualities, aerodynamics, and the flight control system.

Space Shuttle

One of the most noteworthy PID efforts conducted at Dryden over the past 40 years has been with the Space Shuttle Orbiter or space transportation System. For 17 years from 1981 to 1998, shuttle PID analysis was actively conducted at Dryden,[31] not including PID analyses conducted during earlier ALTs in 1977. The Space Shuttle Orbiter provided a one-of-a-kind platform to investigate flight-determined stability and control derivatives for maneuvering flight over a wide range of hypersonic velocities. Stability and control maneuvers were performed in order to safely expand the operational flight envelope via updates to the aerodynamic database and flight control system. That is, PID was justified by operational considerations for space shuttle project support and not by research considerations. Specifically, derivatives were used to determine if certain configuration placards (limitations on the flight envelope) could be modified. Some of these placards involved the longitudinal and lateral c.g. limits used by payload planners and for control system redesign. The placards were determined on the basis of preflight

predictions and the associated uncertainties. As flight-determined derivatives were obtained, the placards were reassessed, and some were modified or removed. The use of PID flight results to update the predicted aerodynamic database of the orbiter is one of the most completely documented processes for a flight vehicle. These updates were modifications to the official aerodynamic database used by the entire space shuttle program for all mission planning, flight critical, and operational purposes. Reference 31 presents a full set of flight-derived stability and control derivatives with comparisons to aerodynamic databook values. Here, we discuss a few interesting results from that report.

The Space Shuttle Orbiter is a large double-delta-winged vehicle designed to reenter the atmosphere and land horizontally. The entry control system consists of 12 vertical reaction control system (RCS) jets (six down firing and six up firing), eight horizontal RCS jets (four to the left and four to the right), four elevon surfaces, a body flap, and a split rudder surface. The vertical jets and elevons control pitch and roll. These jets and elevons are used symmetrically to control pitch and asymmetrically to control roll. Used as a secondary pitch trim control, the body flap helps maintain the predetermined elevon schedule as a function of flight condition. The rudder and side-firing (yaw) jets provide directional control. The split rudder also functions as the speed brake. The vertical jets operate in roll (roll jets) only for dynamic pressures of less than 10 lb/ft^2 and in pitch (pitch jets) for dynamic pressures less than 40 lb/ft^2. The yaw jets are active when the Mach number is greater than one. The body flap and elevons activate at a dynamic pressure of 2 lb/ft^2. The rudders activate at Mach numbers below five.

The predicted stability and control derivatives are given in the preflight aerodynamic data book.[58] These predictions are based on more than 25,000 hours of wind-tunnel testing. The data book also contains estimates of the uncertainty in the predictions. These preflight uncertainties, which are based on an evaluation of previous correlations between wind-tunnel and flight-determined derivatives for similar aircraft,[59] were called the variations. It is essential when comparing flight estimates to predictions that all of the primary flight condition parameters (e.g., Mach number, angle of attack, c.g. location, altitude, and elevon and body flap positions) are interpolated so that the flight values and predicted values are evaluated at the same flight condition.

Maneuvers for stability and control data have been carefully developed to provide the maximum amount of information. It is important to excite the motions that affect the derivatives in question to make them identifiable from the flight data. Because of inherent constraints on the amount of flight testing possible on the space shuttle and maneuver challenges posed by the flight control system (filters, feedback, damping, etc.), precise maneuver design and execution are critical. Programmed test inputs (PTI) were developed to somewhat overcome these problems. Similar to HARV phase II OBES maneuvers, PTI maneuvers are programmed directly into the flight control system via onboard software and are performed at predetermined flight conditions. PTI signals can be sent to the elevon, aileron, and rudder as well as to the pitch, roll, and yaw jets. The input is not completely free of flight control system interference, but the design does allow for enhanced maneuvers. Flight data used for stability and control derivative estimation were recorded on three onboard systems[60] at high sample rates and high resolution to support postflight PID analysis.

The flight data used to update the original preflight aerodynamic data book predictions and uncertainties represented incremental changes to the original data book and were thus called flight assessment deltas or FADs. FADs were generated throughout the shuttle program after various flights and known as FAD–2, −4, −6, −9, −14, and FAD–26, representing successive updates to the aerodynamic data book. Together with the original data book, these FADs constituted the official aerodynamic database used for flying the operational shuttle. These PID results were essential in building the most accurate, up-to-date aerodynamic database to be used exclusively by the government-contractor space shuttle team.

It is informative to consider the challenges of performing an adequate level of PID testing on a vehicle that cannot fly repeated test points in the traditional sense. For purposes of PID, the shuttle collects aerodynamic flight data only between entry interface (400,000 ft) and final approach. Because the shuttle must fly a tight reentry corridor, the matrix of possible flight conditions for PID maneuvers is limited. Several of the estimated stability and control derivatives exhibited a large amount of data scatter (or otherwise large uncertainty bounds) when plotted as functions of Mach number. This behavior can be attributed to a number of causes, not the least of which is that the derivatives are not only functions of Mach number, but of angle of attack, dynamic pressure, altitude, body flap position, and other parameters. Thus, unless all of the maneuvers near a given Mach number share similar flight parameters a two-dimensional plot of derivative vs Mach number will result in data scatter and uncertainty, as was discussed earlier concerning X-29A and F-18 data. That is, much of the scatter is caused by large changes in flight parameters between PID maneuvers. In a typical flight research program, a full matrix of flight condition parameters is specified, and maneuvers performed at the various combinations of parameters and repeated as needed. The orbiter, however, is only able to sparsely populate its test matrix and has scant opportunity to repeat a maneuver, hindering the ability to cross-plot estimated derivatives (e.g., on a carpet plot) and resulting in a significant amount of scatter.

Figure 18 shows the directional stability Cn_β estimated for flights STS-1 through STS-26. In Fig. 18a, the dotted line is the fairing from the preflight aerodynamic data book,[58] and the solid line is the fairing based on the flight-derived estimates from Dryden and affiliated analysts. Each symbol is the Dryden estimate for the PTI maneuver, and vertical bar is the uncertainty level of the estimate; the uncertainty level is 10 times the calculated Cramér–Rao bound. The differences between the fairing of the estimates (solid line) and the Dryden estimates are shown in Fig. 18b as δCn_β, which is defined as

$$\delta Cn_\beta = Cn_{\beta\text{flight}} - (Cn_{\beta\text{databook}} + Cn_{\beta\text{FAD}}) \tag{6}$$

where the databook estimate $Cn_{\beta\text{databook}}$, accounts for all of the maneuver-to-maneuver differences in Mach number, AOA, dynamic pressure, altitude, body flap position, and elevon position.

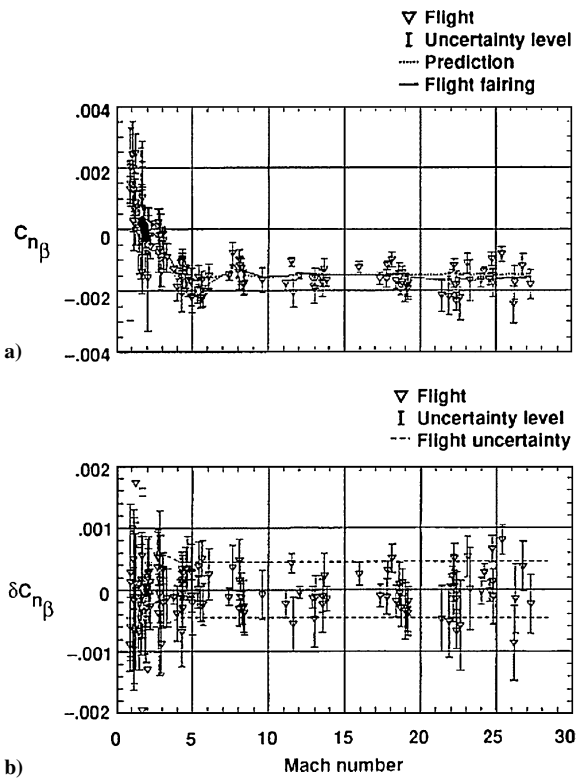

Fig. 18 Space shuttle sideslip derivative as a function of Mach number.

The dashed lines in Fig. 18 show the flight-derived uncertainties of the derivatives. For meaningful interpretation of the results, most of the data should lie between the dashed lines. In particular, the data points with small vertical bounds should be within the dashed lines. As already discussed, data scatter among adjacent estimates is caused largely by differences in flight condition parameters of those estimates (e.g., elevon position and angle of attack; see Ref. 31 for an explanation), rather than randomness or an effect of Mach number.

Significant differences occur between flight and prediction between Mach 1 and 3, between Mach 5 and 6, and above Mach 20. Adjusting the flight simulator to match flight-derived values resulted in improved harmony between the ground-based simulator and the vehicle.

To assess the overall effectiveness of derivative extraction from orbiter flight data, it is instructive to track the evolution (or maturation) of the derivative as a function of the FAD number. We examine the evolution of the directional stability derivative Cn_β for which ΔCn_β from a number of FADs is plotted against Mach number in Fig. 19.

The ΔCn_β fairing for FAD-2 was positive from Mach 1 to Mach 3, negative from Mach 3 to Mach 7, positive from Mach 7 to Mach 13, and negative (and small) above Mach 13. Each succeeding FAD cycle showed the same general pattern of positive and negative increments. However, the size of the increment and the Mach number "switch points" were modified in each succeeding FAD, as increased number of maneuvers were analyzed. As can be seen, the refinement in the FADs is an iterative process with each successive FAD adding more smoothness and detail to ΔCn_β. In FAD-26, ΔCn_β is a fairly smooth curve, with finer changes in the positive and negative increments than earlier versions. This refinement denotes an improved characterization of Cn_β and shows the value of having more PTI maneuvers at a wide variety of flight conditions.

Figure 20 is another illustration of the value of multiple FAD cycles for improving the estimated value of a derivative and specifically, reducing the overall uncertainty range of a derivative. The ΔCl_β is shown with its associated flight-derived uncertainty for FAD-26. The original preflight aerodynamic data book variation for Cl_β is also shown. It can be seen that more maneuvers improve the estimates of the derivative and reduce the flight-derived uncertainty. Although the change in the derivative is quite substantial hypersonically, particularly above Mach 16, the uncertainty in that region is

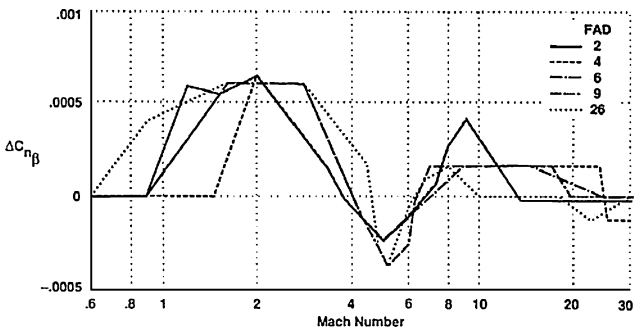

Fig. 19 Fairings of space shuttle ΔCn_β as a function of Mach number.

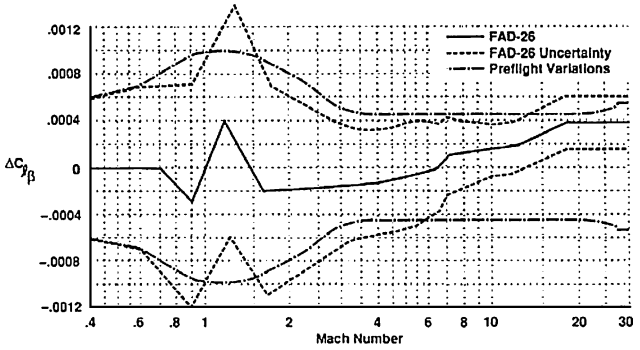

Fig. 20 Fairings of the space shuttle ΔCl_β as a function of Mach number.

reduced 40% of the original, preoperational variation. The combination of the estimate improvement and the uncertainty reduction has a substantial effect on the operational envelope of the vehicle. This fact, coupled with the associated improved robustness of the control system, adds markedly to the overall safety margin of the Space Shuttle Orbiter reentry.[31]

Summary

A brief retrospective of the development of modern parameter identification at NASA Dryden Flight Research Center has been presented. Examples from recent flight programs at Dryden are discussed, and relevant lessons learned are reported. The use of state noise in the Parameter-identification (PID) formulation is shown to be a useful technique in modeling uncommanded responses caused by nonlinear flow phenomena associated with flight at high angles of attack. Consistency in control input amplitude is shown to be important in proper maneuver design because derivatives are locally linear approximations that are sensitive to the amount of angle of attack or sideslip over which a derivative is evaluated. Maneuver quality is greatly enhanced (in terms of repeatability and excitation of state variables) by using preprogrammed single-surface inputs (SSI). Standard doublet maneuvers implementing SSI exhibit good wave-form shape in terms of input amplitude, dwell time, full-cycle duration, and overall square-wave shape. Near-linear dependency problems between correlated controls and feedback effects are largely mitigated with preprogrammed SSIs. There is a need for identifying a minimum amount of highly productive PID flight testing, especially when repeat maneuvers are not readily obtainable. To adequately define derivatives as functions of angle of attack, 10-deg increments between maneuvers are too large, as notable differences can occur over 2- or 3-deg angle of attack, though increments of 5-deg angle of attack are probably sufficient. Proper maneuver planning is essential in reducing data scatter in the estimated derivatives. Experience and engineering judgment are always critical in estimating derivatives, in evaluating the individual estimates, and in properly interpreting the results.

PID has played an integral role in virtually all flight programs at Dryden over the last 40 years. The estimation of stability and control derivatives via flight data has proven essential in updating the aerodynamic database and ground-based simulator. These updates have been used for expanding the operational flight envelope, relaxing flight placards and constraints, revising control system designs, and pilot training to avoid certain undesirable flight conditions. The utility of PID has been clearly demonstrated on numerous flight vehicles investigated at Dryden, with the space shuttle experience being one of the most noteworthy. As long as there are differences between what an aircraft does in the real flight environment and what is modeled or predicted, PID will remain a key flight-test technology for the foreseeable future.

References

[1]Yancey, R. B., "Flight Measurements of Stability and Control Derivatives of the X-15 Research Airplane to a Mach Number of 6.02 and an Angle of Attack of 25 Deg," NASA-TN-D-2532, Nov. 1964.

[2]Smith, H. J., "Evaluation of the Lateral-Directional Stability and Control Characteristics of the Lightweight M2-F1 Lifting Body at Low Speeds," NASA TN-D-3022, Sept. 1965.

[3]Wolowicz, C. H., "Considerations in the Determination of Stability and Control Derivatives and Dynamic Characteristics from Flight Data," AGARD-AR-549, Pt. 1, 1966.

[4]Rampy, J. M., and Barry, D. T., "Determination of Stability Derivatives from Flight Test Data by Means of High Speed Repetitive Operation Analog Matching," Air Force Flight Test Center, FTC-TDR-64-8, Edwards AFB, CA, May 1964.

[5]Howard, J., "The Determination of Lateral Stability and Control Derivatives from Flight Data," *Canadian Aeronautics Space Journal*, Vol. 13, No. 3, 1967, pp. 126–134.

[6]Shinbrot, M., "On the Analysis of Linear and Non-Linear Dynamical Systems from Transient Response Data," NACA TN-3288, Dec. 1954.

[7]Greenberg, H., "A Survey of Methods for Determining Stability Parameters of an Airplane From Dynamic Flight Measurement," NACA TN-2340, April 1951.

[8]Breuhaus, W. O., "Summary of Dynamic Stability and Control Flight Research Conducted Utilizing a B-25J Airplane," Cornell Aeronautical Lab., Rept. TB-405-F-10, Buffalo, New York, May 1948.

[9]Seamans, R. C., Jr., Blasingame, B. P., and Clementson, G. C., "The Pulse Method for the Determination of Aircraft Dynamic Performance," *Journal of the Aeronautical Sciences*, Vol. 17, No. 1, 1950, pp. 22–38.

[10]Rynaski, E. G., "Application of Advanced Identification Techniques to Nonlinear Equations of Motion," *Proceedings of the Stall/Post-Stall/Spin Symposium*, Wright–Patterson Air Force Base, Ohio, Dec. 1971, pp. 0-1–0-18.

[11]Iliff, K. W., and Taylor, L. W., Jr., "Determination of Stability Derivatives from Flight Data Using a Newton-Raphson Minimization Technique," NASA TN D-6579, 1972.

[12]Balakrishnan, A. V., *Communication Theory*, McGraw–Hill, New York, 1968.

[13]Balakrishnan, A. V., "Stochastic System Identification Techniques," *Stochastic Optimization and Control*, edited by H. F. Karreman, Wiley, London, 1968.

[14]Taylor, L. W., Jr., and Iliff, K. W., "A Modified Newton-Raphson Method for Determining Stability Derivatives from Flight Data," *Second International Conference on Computing Methods in Optimization Problems*, Academic Press, New York, 1969, pp. 353–364.

[15]Taylor, L. W., Jr., Iliff, K. W., and Powers, B. G., "A Comparison of Newton-Raphson and Other Methods for Determining Stability Derivatives from Flight Data," Third Technical Workshop on Dynamic Stability Problems, NASA Ames Research Center, Moffett Field, CA, Nov. 1968.

[16]Iliff, K. W., Powers, B. G., and Taylor, L. W., Jr., "A Comparison of Newton-Raphson and Other Methods for Determining Stability Derivatives from Flight Data," AIAA Paper 69-315, March 1969.

[17]Norton, F. H., "The Measurement of the Damping in Roll on a JN4h in Flight," NACA Rept. 167, 1923.

[18]Norton, F. H., "A Study of Longitudinal Dynamic Stability in Flight," NACA Rept. 170, 1923.

[19]Balakrishnan, A. V., "Stochastic Differential System I," *Filtering and Control; A Function Space Approach*, edited by M. Beckman, G. Goos, and H. P. Kunzi, Lecture Notes in Economics and Mathematical Systems, Vol. 84, Springer-Verlag, Berlin, 1973.

[20]Iliff, K. W., "Maximum Likelihood Estimates of Lift and Drag Characteristics Obtained from Dynamic Aircraft Maneuvers," *Proceedings of the AIAA 3rd Atmospheric Flight Mechanics Conference*, AIAA, New York, 1976, pp. 137–150; also *Journal of Aircraft*, Vol. 14, No. 12, 1977, pp. 1175–1181.

[21]Edwards, J. W., "Flight Test Results of an Active Flutter Suppression System Installed on a Remotely Piloted Research Vehicle," NASA TM-83132, 1981.

[22]Iliff, K. W., and Wang, K. C., "Flight-Determined Subsonic Longitudinal Stability and Control Derivatives of the F-18 High Angle of Attack Research Vehicle (HARV) with Thrust Vectoring," NASA TP-97-206539, Dec. 1997.

[23]Iliff, K. W., and Wang, K. C., "Flight-Determined Subsonic Lateral-Directional Stability and Control Derivatives of the Thrust-Vectoring F-18 High Angle of Attack Research Vehicle (HARV), and Comparisons to the Basic F-18 and Predicted Derivatives," NASA TP-99-206573, Jan. 1999.

[24]Iliff, K. W., Maine, R. E., and Shafer, M. F., "Subsonic Stability and Control Derivatives for an Unpowered, Remotely Piloted 3/8-Scale F-15 Airplane Model Obtained From Flight Test," NASA TN-D-8136, Jan. 1976.

[25]Iliff, K. W., "Identification and Stochastic Control with Application to Flight Control in Turbulence," Ph.D. Dissertation, UCLA-ENG-7430, Univ. of California, Los Angeles, May 1973.

[26]Iliff, K. W., "Estimation of Characteristics and Stochastic Control of an Aircraft Flying in Atmospheric Turbulence," *Proceedings of the AIAA 3rd Atmospheric Flight Mechanics Conference*, AIAA, New York, 1976, pp. 26–38; also *Journal of Guidance and Control*, Vol. 1, No. 2, 1978, pp. 101–108.

[27]Maine, R. E., and Iliff, K. W., "User's Manual for MMLE3, A General FORTRAN Program for Maximum Likelihood Parameter Estimation," NASA TP-1563, Nov. 1980.

[28]Maine, R. E., "Programmer's Manual for MMLE3, A General FORTRAN Program for Maximum Likelihood Parameter Estimation," NASA TP-1690, June 1981.

[29]Cooke, D. R., "Minimum Testing of the Space Shuttle Orbiter for Stability and Control Derivatives," *Shuttle Performance: Lessons Learned*, edited by J. P. Arrington and J. J. Jones, NASA Langley Research Center, NASA CP-2283, Hampton, VA, Pt. 1, 1983, pp. 447–471.

[30]Kirsten, P. W., Richardson, D. F., and Wilson, C. M., "Predicted and Flight Test Results of the Performance, Stability and Control of the Space Shuttle From Reentry to Landing," *Shuttle Performance: Lessons Learned*, edited by J. P. Arrington and J. J. Jones, NASA Langley Research Center, NASA CP-2283, Hampton, VA, Pt. 1, 1983, pp. 509–524.

[31]Iliff, K. W., and Shafer, M. F., "Extraction of Stability and Control Derivatives from Orbiter Flight Data," NASA TM-4500, June 1993.

[32]Murray, J. E., and Maine, R. E., "The pEst Version 2.1 User's Manual," NASA TM-88280, Sept. 1987.

[33]Hamel, P. G., and Jategaonkar, R. V., "Evolution of Flight Vehicle System Identification," *Journal of Aircraft*, Vol. 33, No. 1, 1996, pp. 9–28.

[34]Weiss, S., Friehmelt, F. H., Plaetschke, E., and Rohlf, D., "X-31A System Identification Using Single-Surface Excitation at High Angles of Attack," *Journal of Aircraft*, Vol. 33, No. 3, 1996, pp. 485–490.

[35]Klein, V., "Maximum Likelihood Method for Estimating Airplane Stability and Control Parameters From Flight Data in Frequency Domain," NASA TP-1637, 1980.

[36]Morelli, E. A., "Practical Input Optimization for Aircraft Parameter Estimation Experiments," NASA CR-191242, May 1993.

[37]Klein, V., "On the Adequate Model for Aircraft Parameter Estimation," Cranfield Inst. of Technology, Cranfield Rept. Aero No. 28, England, U.K., March 1975.

[38]Tischler, M. B., "System Identification Methods for Aircraft Flight Control Development and Validation," NASA TM-110369, Oct. 1995.

[39]Maine, R. E., and Iliff, K. W., "The Theory and Practice of Estimating the Accuracy of Dynamic Flight-Determined Coefficients," NASA RP-1077, July 1981.

[40]Maine, R. E., and Iliff, K. W., "Identification of Dynamic Systems, Theory and Formulation," NASA RP-1138, Feb. 1985; also AGARD-AG-300, Vol. 2, 1985.

[41]Maine, R. E., and Iliff, K. W., "Application of Parameter Estimation to Aircraft Stability and Control: The Output-Error Approach," NASA RP-1168, June 1986.

[42]Iliff, K. W., "Aircraft Parameter Estimation," NASA TM-88281, Jan. 1987; also AIAA Paper CP-87-0623, Jan. 1987.

[43]Maine, R. E., and Iliff, K. W., "Formulation and Implementation of a Practical Algorithm for Parameter Estimation with Process and Measurement Noise," *SIAM Journal of Applied Mathematics*, Vol. 41, 1981, pp. 558–579.

[44]Iliff, K. W., and Maine, R. E., "Practical Aspects of Using a Maximum Likelihood Estimation Method to Extract Stability and Control Derivatives from Flight Data," NASA TN D-8209, April 1976.

[45]Iliff, K. W., Maine, R. E., and Montgomery, T. D., "Important Factors in the Maximum Likelihood Analysis of Flight Test Maneuvers," NASA TP-1459, April 1979.

[46]Iliff, K. W., and Maine, R. E., "More Than You May Want to Know About Maximum Likelihood Estimation," AIAA CP-84-2070, Aug. 1984; also NASA TM-85905, Jan. 1985.

[47]Maine, R. E., and Murray, J. E., "Application of Parameter Estimation to Highly Unstable Aircraft," NASA TM-88266, Aug. 1986.

[48]Iliff, K. W., and Maine, R. E., "Bibliography for Aircraft Parameter Estimation," NASA TM-86804, Oct. 1986.

[49]Iliff, K. W., and Wang, K. C., "X-29A Lateral-Directional Stability and Control Derivatives from High-Angle-of-Attack Flight Data," NASA TP-3664, Dec. 1996.

[50]Iliff, K. W., and Wang, K. C., "Extraction of Lateral-Directional Stability and Control Derivatives for the Basic F-18 Aircraft at High Angles of Attack," NASA TM-4786, Feb. 1997.

[51]Moes, T. R., and Iliff, K. W., "Stability and Control Estimation Flight Test Results for the SR-71 Aircraft With Externally Mounted Experiments," NASA TP-2002-210718, June 2002.

[52]Moes, T. R., Cobleigh, B. R., Cox, T. H., Conners, T. R., Iliff, K. W., and Powers, B. G., "Flight Stability and Control and Performance Results from the Linear Aerospike SR-71 Experiment (LASRE)," NASA TM-1998-206565, Aug. 1998; also AIAA Paper CP-98-4340, Aug. 1998.

[53]Klein, V., Ratvasky, T. P., and Cobleigh, B. R., "Aerodynamic Parameters of High Angle-of-Attack Research Vehicle (HARV) Estimated from Flight Data," NASA TM-102692, Aug. 1990.

[54]Bowers, A. H., and Pahle, J. W., "Thrust Vectoring on the NASA F-18 High Alpha Research Vehicle," NASA TM-4771, Nov. 1996.

[55]"F/A-18 Basic Aerodynamic Data," McDonnell Aircraft Co., McDonnell Douglas Corp., MDC A8575, St. Louis, MO, 1984.

[56]Pelikan, R. J., and Swingle, R. L., "F/A-18 Stability and Control Data Report," McDonnell Aircraft Co., McDonnell Douglas Corp., Vols. I and II, MDC A7247, Rev. B, St. Louis, MO, Nov. 1982.

[57]Moes, T. R., Noffz, G. K., and Iliff, K. W., "Results From F-18B Stability and Control Parameter Estimation Flight Tests at High Dynamic Pressures," NASA TP-2000-209033, Nov. 2000.

[58]"Aerodynamic Design Data Book Orbiter Vehicle STS-1," Rockwell International, Space Div., Downey, CA, SD71-5H-0060 Rev. M, Downey, CA, Nov. 1980.

[59]Weil, J., and Powers, B. G., "Correlation of Predicted and Flight Determined Stability and Control Derivatives—with Particular Application to Tailless Delta Wing Configurations," NASA TM-81361, July 1981.

[60]Throckmorton, D. A., "Shuttle Entry Aerothermodynamic Flight Research: The Orbiter Experiments (OEX) Program," AIAA Paper CP-92-3987, July 1992.